Pergamon

Int. J. Heat Mass Transfer. Vol. 39, No. 8, pp. 1625–1637, 1996

0017-9310/96 $15.00 + 0.00

0017-9310(95)00266-9

An extract analytical solution for the extended turbulent Graetz problem with Dirichlet wall boundary conditions for pipe and channel flows

B. WEIGAND

ABB Power Generation Ltd, Gas Turbine Development, 5401 Baden, Switzerland

(*Received* 21 *March* 1995 *and in final form* 29 *June* 1995)

Abstract—For turbulent flows in ducts axial heat conduction effects within the fluid can be important for low Prandtl number fluids (liquid metals). The paper presents an entirely analytical solution to the extended turbulent Graetz problem with Dirichlet wall boundary conditions. The solution is based on a selfadjoint formalism resulting from a decomposition of the convective diffusion equation for turbulent flow into a pair of first-order partial differential equations. The present approach, which is based on the solution method of Papoutsakis *et al.* for laminar pipe flow, is not plagued by any uncertainties arising from expansions in terms of eigenfunctions belonging to a nonselfadjoint operator. The obtained analytical results are compared with measurements of Gilliland *et al.* and Sleicher *et al.* showing good agreement between measured and predicted values.

1. INTRODUCTION

The relative importance of axial conduction in heat transfer to a fluid flowing inside a duct depends primarily on the magnitude of the Peclet number. For laminar flow through a circular pipe, for instance, axial heat conduction in the fluid can be neglected in comparison to radial conduction if the Peclet number exceeds approximately 100. The classical Graetz problem deals with heat transfer in the developing thermal region under such conditions [1–3]. However, for flows with Peclet numbers smaller than 100, axial heat conduction in the fluid becomes increasingly important as Pe_D decreases. This is the case, for example, in compact heat exchangers where liquid metals are used as the working fluids.

In the past many investigations have been carried out which deal with the solution of the extended Graetz problem (the Graetz problem considering axial heat conduction in the fluid) for thermally developing laminar flow in a pipe or in a parallel plate channel. Extensive literature reviews on this subject are given in [4] and [5]. Many of the solutions cited in [4, 5] for the extended Graetz problem are based on the fundamental assumption that the solution of the problem has the same form of the series solution as the Graetz problem without axial heat conduction in the fluid. This approach results in a nonselfadjoint eigenvalue problem with eigenvalues that could, at least in principle, be complex and eigenvectors that could be incomplete. Several strategies have been developed in the past to overcome this problem. Hsu [6] constructed the solution of the problem from two independent series solutions for $x < 0$ and $x > 0$. Both the temperature distribution and the temperature gradient were then matched at $x = 0$ by constructing a pair of orthonormal functions from the nonorthogonal eigenfunctions by using the Gram–Schmidt-orthonormalization procedure. Hence this method is clearly plagued with the uncertainties arising from expansion in terms of eigenfunctions and eigenvalues belonging to a nonselfadjoint operator. It was the merit of Papoutsakis *et al.* [7] to show that it is possible to produce an entirely analytical solution to the extended Graetz problem for Dirichlet boundary conditions. Their solution is based on a selfadjoint formalism resulting from a decomposition of the convective diffusion equation into a pair of first-order partial differential equations. The method was originated by Ramkrishna and Amundson [8]. Later a different approach for obtaining an analytical solution of the extended Graetz problem was presented by Ebadian and Zhang [9]. They used a Fourier transform of the temperature field and expanded the coefficients of the transformed temperature in terms of the Peclet number. This approach resulted in a set of ordinary differential equations which can be solved successively.

Additionally several investigations have been carried out in the past concerning the extended Graetz problem in a parallel plate channel. Deavours [10] presented an analytical solution for the extended Graetz problem by decomposing the eigenvalue problem for the parallel plate channel into a system of ordinary differential equations for which he proved the orthogonality of the eigenfunctions. Weigand *et al.* [11] studied liquid solidification in a parallel plate channel subjected to laminar internal flow. They applied a regular perturbation expansion to the energy equation. The zero order problem was formally identical

NOMENCLATURE

a	thermal diffusivity
a_1, a_2	functions defined by equations (11) and (12)
A_j	constants
c_p	specific heat at constant pressure
D	hydraulic diameter, $4h$ (planar channel), $2R$ (circular pipe)
$\mathbf{f}$, $\mathbf{F}$	vectors
ΔF	relative error, $(Nu_{\text{elliptic}} - Nu_{\text{parabolic}})/Nu_{\text{elliptic}}$
h	distance between the centerline and the wall (planar duct)
k	flow index, 0 for a planar channel, 1 for a circular pipe
k	thermal conductivity
l	mixing length
L	characteristic length, $L = h$ (planar duct), $L = R$ (circular pipe)
$\mathbf{L}$	matrix operator, equation (15)
n	coordinate
Nu_D	Nusselt number based on the hydraulic diameter, equation (41)
Nu_∞	Nusselt number for fully-developed flow, equation (47)
P	pressure
Pr	Prandtl number
Pe_L	Peclet number based on the characteristic length L
Pe_D	Peclet number based on the hydraulic diameter
Pr_t	turbulent Prandtl number
r	radial coordinate
R	pipe radius
Re_L	Reynolds number based on the characteristic length L
Re_D	Reynolds number based on the hydraulic diameter
T	temperature
T_0	uniform temperature for $x \to \infty$
T_F	uniform temperature for $x \to -\infty$
T_b	bulk temperature, equation (42)
u	axial velocity
$\bar{u}_0$	axial mean velocity
u_τ	friction velocity, $\sqrt{(\tau_{nx})_w/\rho}$
x	axial coordinate
y^+	wall coordinate, $u_\tau(L-n)/\nu$.

Greek symbols

ε_{hx}	eddy diffusivity in axial direction
ε_{hn}	eddy diffusivity in normal direction
ε_m	eddy kinematic viscosity
ρ	density
λ_j	eigenvalue
θ	dimensionless temperature
θ_b	dimensionless bulk temperature
$\lvert \tau_{nx} \rvert_w$	wall shear stress
ν	kinematic viscosity
Σ	axial energy flow, equation (13)
$\mathbf{\Phi}_j$	eigenfunction.

with the extended Graetz problem in a parallel plate channel. For the solution of the zero order problem they followed the method of Papoutsakis *et al.* [7] and obtained an analytical solution. There are many numerical investigations which deal with the extended Graetz problem for laminar flow in a pipe or a parallel plate channel, for example [12, 13]. For more detailed information concerning numerical investigations the reader is referred to [4, 5].

Although axial heat conduction can be ignored for turbulent convection in ordinary fluids and gases, with liquid metals this might not always be justified. In fact because of the very low Prandtl numbers for liquid metals ($0.001 < Pr < 0.06$) the Peclet number can be as small as three in turbulent duct flows. A literature review about the convective heat transfer in liquid metals can be found in [5]. Lee [14] studied the extended Graetz problem in turbulent pipe flow. He found that for Peclet numbers below 100, axial heat conduction in the fluid becomes important in the thermal entrance region. He investigated a pipe which was insulated for $x < 0$ and had a uniform wall temperature for $x > 0$. Lee used the method of Hsu [6] to obtain a series solution for the problem. In [14] the variation of the Nusselt number for fully-developed flow was shown for several Peclet and Prandtl numbers. In addition the error in Nusselt number resulting from neglecting the axial heat conduction effect was presented. This error was found to be as much as 40% for a Peclet number of 5. A shortcoming of [14] is that no eigenvalues or constants were presented for various Peclet and Prandtl numbers. Also, no variations of the Nusselt number in the thermal entrance region were shown.

No investigation is known in the literature which deals with the effect of axial heat conduction in a turbulent flowing liquid inside a pipe with Dirichlet boundary conditions (wall temperature of the pipe specified for $x < 0$ and $x > 0$ with a step in the wall temperature for $x = 0$). For the case of turbulent flow inside a parallel plate channel, the effect of axial heat conduction within the fluid was only studied by Faggiani and Gori [22]. They solved numerically the energy equation for a constant heat flux boundary condition. No investigation is known in literature which deals with the effect of axial heat conduction in a parallel plate channel for the case of prescribed wall temperature boundary conditions. Additionally, there

is no analytical investigation known which studies the effect of axial heat conduction within a parallel plate channel for turbulent flow.

Therefore, the purpose of the present paper is to derive an exact analytical solution for the extended Graetz problem with Dirichlet wall boundary conditions for turbulent flows with low Peclet numbers inside a parallel plate channel as well as a circular pipe. By using a solution method similar to Papoutsakis *et al.* [7] it is possible to derive, with the help of a newly defined vector norm, analytical solutions for the extended Graetz problem which are computationally as simple and efficient as the solution of the parabolic problem. In addition, the solution presented here is not plagued with any uncertainties arising from expansions in terms of eigenfunctions belonging to a nonselfadjoint operator.

2. ANALYSIS

Figure 1 shows the geometrical configuration and the coordinate system. The characteristic length L denotes half of the channel height h for the flow in a parallel plate channel or the radius R for the flow in a circular pipe. It is assumed that the flow enters the duct with a fully-developed turbulent velocity profile and with a uniform temperature profile T_0 for $x \to -\infty$. For $x \to +\infty$ the flow will attain the uniform temperature. T_F. The wall temperature is maintained at T_0 for $x \leqslant 0$ and at T_F for $x > 0$. Under the assumptions of an incompressible flow with constant physical properties, negligible viscous and turbulent energy dissipation and hydrodynamically fully-developed flow, the energy equation is given by

$$\rho c_p u \frac{\partial T}{\partial x} = \frac{\partial}{\partial x}\left[(k+\rho c_p \varepsilon_{hx})\frac{\partial T}{\partial x}\right] + \frac{1}{r^k}\frac{\partial}{\partial n}\left[r^k(k+\rho c_p \varepsilon_{nn})\frac{\partial T}{\partial n}\right] \quad (1)$$

with the boundary conditions

$$n = L\colon T = T_0, x \leqslant 0 \quad \text{and} \quad T = T_F, x > 0$$
$$n = 0\colon \partial T/\partial n = 0, \quad \lim_{x\to-\infty} T = T_0, \quad \lim_{x\to+\infty} T = T_F. \quad (2)$$

The index k which appears in equation (1) is equal to 0 for a planar duct and equal to 1 for a circular pipe. The velocity distribution u which appears in equation (1) has been calculated from the momentum equation for hydrodynamically fully-developed flow

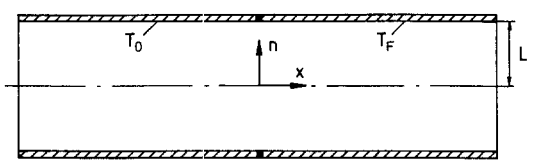

Fig. 1. Geometrical configuration and coordinate system.

$$\frac{\partial P}{\partial x} = \frac{1}{r^k}\frac{\mathrm{d}}{\mathrm{d}n}\left[r^k(\mu+\varepsilon_m)\frac{\mathrm{d}u}{\mathrm{d}n}\right] \quad (3)$$

with the boundary conditions

$$n = 0\colon \frac{\mathrm{d}u}{\mathrm{d}n} = 0 \quad n = L\colon u = 0. \quad (4)$$

Additionally the conservation of mass in integral form

$$\bar{u}_0 L^{2k+1} = \frac{1}{k+1}\int_0^L u r^k \,\mathrm{d}n \quad (5)$$

has to be satisfied. This equation determines the unknown pressure drop in the duct. The eddy viscosity ε_m in equation (3) is modelled by using the well-known Nikuradse mixing length formula with the van Driest damping factor

$$\varepsilon_m = l^2\left|\frac{\mathrm{d}u}{\mathrm{d}n}\right| \quad (6)$$

with l given by

$$l = L\left[0.14 - 0.08\left(\frac{n}{L}\right)^2 - 0.06\left(\frac{n}{L}\right)^4\right](1-\exp(-y^+/26)). \quad (7)$$

By introducing the following dimensionless quantities

$$\theta = \frac{T-T_F}{T_0-T_F} \quad \tilde{x} = \frac{x}{L}\frac{1}{Pe_L} \quad \tilde{u} = \frac{u}{\bar{u}_0}$$
$$\tilde{n} = \frac{n}{L} \quad \tilde{r} = \frac{r}{L} \quad Pe_L = Re_L Pr,$$
$$Re_L = \frac{\bar{u}_0 L}{\nu} \quad Pr = \frac{\nu}{a}$$
$$\tilde{\varepsilon}_m = \frac{\varepsilon_m}{\nu} \quad Pr_t = \frac{\varepsilon_m}{\varepsilon_{hn}} \quad (8)$$

into equations (1) and (2) the energy equation can be cast into the following nondimensional form

$$\tilde{u}\frac{\partial\theta}{\partial\tilde{x}} = \frac{1}{Pe_L^2}\frac{\partial}{\partial\tilde{x}}\left[a_1\frac{\partial\theta}{\partial\tilde{x}}\right] + \frac{1}{\tilde{r}^k}\frac{\partial}{\partial\tilde{n}}\left[r^k a_2\frac{\partial\theta}{\partial\tilde{n}}\right] \quad (9)$$

with the boundary conditions

$$\tilde{n} = 1\colon \theta = 1, x \leqslant 0 \quad \text{and} \quad \theta = 0, x > 0;$$
$$\tilde{n} = 0\colon \partial\theta/\partial\tilde{n} = 0 \quad \lim_{\tilde{x}\to-\infty}\theta = 1 \quad \lim_{\tilde{x}\to+\infty}\theta = 0. \quad (10)$$

The functions $a_1(\tilde{n})$ and $a_2(\tilde{n})$ are given by

$$a_1(\tilde{n}) = 1 + \frac{Pr}{Pr_t}\tilde{\varepsilon}_m\left(\frac{\varepsilon_{hx}}{\varepsilon_{hn}}\right) \quad (11)$$

$$a_2(\tilde{n}) = 1 + \frac{Pr}{Pr_t}\tilde{\varepsilon}_m. \quad (12)$$

In the following solution process for equation (9) no assumptions are required about the functions $a_1(\tilde{n})$ and $a_2(\tilde{n})$. The solution presented here holds for arbitrary functions $a_1(\tilde{n})$ and $a_2(\tilde{n})$ as long as $a_1 \geqslant 1, a_2 \geqslant 1$ which is obviously true from the structure of equations (11) and (12). Therefore, the turbulent Prandtl number as well as the ratio $\varepsilon_{hx}/\varepsilon_{hn}$ which were used in the equations (11) and (12) will be specified later.

Papoutsakis *et al.* [7] showed that it is possible to solve equation (9) for laminar pipe flow ($a_1 = a_2 = 1$) by decomposing the elliptic partial differential equation into a pair of first order partial differential equations. The ensuing procedure for solving the extended turbulent Graetz problem given by equations (9) and (10) follows the method of Papoutsakis *et al.* [7] for deriving the solution of the more general problem where a_1 and a_2 are functions of $\tilde{n}$.

Let us define a function $\Sigma(\tilde{x}, \tilde{n})$ which may be called the axial energy flow through a cross-sectional area of the height $\tilde{n}$ by

$$\Sigma = \int_0^{\tilde{n}} \left[\tilde{u}\theta - \frac{1}{Pe_L^2} a_1(\tilde{n}) \frac{\partial \theta}{\partial \tilde{x}} \right] \tilde{r}^k \, \mathrm{d}\tilde{n}. \tag{13}$$

Introducing Σ, defined by equation (13), into the energy equation (9) results in the following system of partial differential equations

$$\frac{\partial}{\partial \tilde{x}} \mathbf{F}(\tilde{x}, \tilde{n}) = \mathbf{L}\mathbf{F}(\tilde{x}, \tilde{n}) \tag{14}$$

with the two component vector $\mathbf{F}$ and the operator $\mathbf{L}$ given by

$$\mathbf{F} = \begin{bmatrix} \theta(\tilde{x}, \tilde{n}) \\ \Sigma(\tilde{x}, \tilde{n}) \end{bmatrix}$$

$$\mathbf{L} = \begin{bmatrix} \dfrac{Pe_L^2 \tilde{u}}{a_1(\tilde{n})} & -\dfrac{Pe_L^2}{\tilde{r}^k a_1(\tilde{n})} \dfrac{\partial}{\partial \tilde{n}} \\ \tilde{r}^k a_2(\tilde{n}) \dfrac{\partial}{\partial \tilde{n}} & 0 \end{bmatrix}. \tag{15}$$

The boundary conditions belonging to $\Sigma(\tilde{x}, \tilde{n})$ can be derived from equation (10) and equation (13)

$$\lim_{\tilde{x} \to -\infty} \Sigma = \int_0^{\tilde{n}} \tilde{u} \tilde{r}^k \, \mathrm{d}\tilde{n} \quad \lim_{\tilde{x} \to \infty} \Sigma = 0 \quad \tilde{n} = 0 : \Sigma = 0. \tag{16}$$

Before calculating the solution of equation (9), some interesting details about the operator $\mathbf{L}$ and the corresponding eigenvalue problem for equation (14) should be presented. The most remarkable aspect of $\mathbf{L}$ is that it gives rise to a selfadjoint problem even though the original convective diffusion operator is nonselfadjoint. This fact is of course dependent on the sort of inner product between two vectors which will be used. If we define an inner product between two vectors

$$\mathbf{\Phi} = \begin{bmatrix} \Phi_1(\tilde{n}) \\ \Phi_2(\tilde{n}) \end{bmatrix} \quad \mathbf{\Lambda} = \begin{bmatrix} \Lambda_1(\tilde{n}) \\ \Lambda_2(\tilde{n}) \end{bmatrix} \tag{17}$$

as

$$\langle \mathbf{\Phi}, \mathbf{\Lambda} \rangle = \int_0^1 \left[\frac{a_1(\tilde{n}) \tilde{r}^k}{Pe_L^2} \Phi_1(\tilde{n}) \Lambda_1(\tilde{n}) + \frac{1}{a_2(\tilde{n}) \tilde{r}^k} \Phi_2(\tilde{n}) \Lambda_2(\tilde{n}) \right] \mathrm{d}\tilde{n} \tag{18}$$

and the following domain for $\mathbf{L}$

$$D(\mathbf{L}) = \{ \mathbf{\Phi} \in H : \mathbf{L}\mathbf{\Phi} \text{ (exists and)} \in H, \Phi_1(1) = \Phi_2(0) = 0 \} \tag{19}$$

then it can be shown that $\mathbf{L}$ is a symmetric operator in the Hilbert space H of interest (this means that $\langle \mathbf{\Phi}, \mathbf{L}\mathbf{\Lambda} \rangle = \langle \mathbf{L}\mathbf{\Phi}, \mathbf{\Lambda} \rangle$). The general expression for the inner product given by equation (18) was developed by the author. This expression reduces for laminar pipe flow ($k = 1$, $a_1 = a_2 1 = 1$) to the inner product given by Papoutsakis *et al.* [7] and for $k = 0$, $a_1 = a_2 = 1$ to the inner product given by Weigand *et al.* [11] for laminar flow and heat transfer in a parallel plate channel. Thus the selfadjoint eigenvalue problem associated with equation (14) is given by

$$\mathbf{L}\mathbf{\Phi}_j = \lambda_j \mathbf{\Phi}_j \tag{20}$$

where $\mathbf{\Phi}_j$ denotes the eigenvector corresponding with the eigenvalue λ_j. Using the definition of the matrix operator $\mathbf{L}$ given by equation (15), the eigenvalue problem, equation (20), can be rewritten in the form

$$Pe_L^2 \left[\frac{\tilde{u}}{a_1(\tilde{n})} \Phi_{j1} - \frac{1}{\tilde{r}^k a_1(\tilde{n})} \Phi'_{j2} \right] = \lambda_j \Phi_{j1} \tag{21}$$

$$\tilde{r}^k a_2(\tilde{n}) \Phi'_{j1} = \lambda_j \Phi_{j2}. \tag{22}$$

If Φ_{j2} is eliminated from equation (22), the following eigenvalue problem for Φ_{j1} can be obtained

$$[\tilde{r}^k a_2(\tilde{n}) \Phi'_{j1}]' + \tilde{r}^k \left[\frac{\lambda_j a_1(\tilde{n})}{Pe_L^2} - \tilde{u} \right] \lambda_j \Phi_{j1} = 0. \tag{23}$$

Equation (23) has to be solved in conjunction with the boundary conditions

$$\Phi'_{j1}(0) = 0 \quad \Phi_{j1}(1) = 0. \tag{24}$$

Additionally an arbitrary normalizing condition

$$\Phi_{j1}(0) = 1 \tag{25}$$

has been used for the eigenvectors. Equation (23) possesses both positive eigenvalues λ_j^+ with the corresponding eigenvectors Φ_j^+ and negative eigenvalues λ_j^- with eigenvectors Φ_j^-. This is because the operator $\mathbf{L}$ is neither positive nor negative definite. All λ_j are real because they are in fact the eigenvalues of a selfadjoint problem. For $a_1(\tilde{n})/Pe_L^2 \to 0$ the eigenvalue problem given by equation (23) reduces to the parabolic Graetz problem in turbulent flow. For $a_1 = a_2 = 1$ and a lami-

nar velocity profile for $\tilde{u}$ the eigenvalue problem reduces to the extended Graetz problem for laminar flow.

Because the two sets of eigenvectors, normalized according to equation (25), constitute an orthonormal basis in H (see Appendix 1) an arbitrary vector $\mathbf{f}$ can be expanded in terms of eigenfunctions in the following way

$$\mathbf{f} = \sum_{j=1}^{\infty} \langle f, \mathbf{\Phi}_j \rangle / \| \mathbf{\Phi}_j \|^2 \mathbf{\Phi}_j(\tilde{n}) \tag{26}$$

with the vector norm $\| \mathbf{\Phi}_j \|^2 = \langle \mathbf{\Phi}_j, \mathbf{\Phi}_j \rangle$. If we explicitly distinguish in equation (26) between positive and negative eigenvectors, equation (26) takes the following form

$$\mathbf{f} = \sum_{j=1}^{\infty} \frac{\langle \mathbf{f}, \mathbf{\Phi}_j^+ \rangle}{\| \mathbf{\Phi}_j^+ \|^2} \mathbf{\Phi}_j^+(\tilde{n}) + \sum_{j=1}^{\infty} \frac{\langle \mathbf{f}, \mathbf{\Phi}_j^- \rangle}{\| \mathbf{\Phi}_j^- \|^2} \mathbf{\Phi}_j^-(\tilde{n}). \tag{27}$$

Now let us reconsider the solution of equation (14). The solution of the problem $\mathbf{F}(\tilde{x}, \tilde{n})$ will be obtained in the form of the series given in equation (27). Therefore, the inner product appearing in the expansion coefficients of equation (27) must be determined. Using equation (18), it can be seen that

$$\langle \mathbf{LF}, \mathbf{\Phi}_j \rangle = \langle \mathbf{F}, \mathbf{L\Phi}_j \rangle + \Phi_{j2}(1) g(\tilde{x}). \tag{28}$$

The function $g(\tilde{x})$ is given by

$$g(\tilde{x}) = \begin{cases} 1, & \tilde{x} \leqslant 0 \\ 0, & \tilde{x} > 0. \end{cases} \tag{29}$$

Taking the inner product of both sides of equation (14) with Φ_j and using equation (28) one obtains with the help of equation (20)

$$\frac{\partial}{\partial \tilde{x}} \langle \mathbf{F}, \mathbf{\Phi}_j \rangle = \lambda_j \langle \mathbf{F}, \mathbf{\Phi}_j \rangle + g(\tilde{x}) \Phi_{j2}(1). \tag{30}$$

Equation (30) can be solved separately for positive and negative eigenvalues. This results in

$$\langle \mathbf{F}, \mathbf{\Phi}_j^- \rangle = C_{0j}^- \exp(\lambda_j^- \tilde{x}) + \int_{-\infty}^{\tilde{x}} (g(\bar{x}) \Phi_{j2}^-(1)) \exp(\lambda_j^- (\tilde{x} - \bar{x}))\, \mathrm{d}\bar{x} \tag{31}$$

$$\langle \mathbf{F}, \mathbf{\Phi}_j^+ \rangle = C_{0j}^+ \exp(\lambda_j^+ \tilde{x}) - \int_{\tilde{x}}^{\infty} (g(\bar{x}) \Phi_{j2}^+(1)) \exp(\lambda_j^+ (\tilde{x} - \bar{x}))\, \mathrm{d}\bar{x}. \tag{32}$$

Because the solution must be bounded for $\tilde{x} \to +\infty$ and for $\tilde{x} \to -\infty$, the two constants C_{0j}^- and C_0^+, appearing in the equations (31) and (32) must be zero. After carrying out the integrations in equations (31) and (32) the following results for $\theta(\tilde{x}, \tilde{n})$, which is the first vector component of $\mathbf{F}(\tilde{x}, n)$, can be derived

$$\tilde{x} \leqslant 0: \theta(\tilde{x}, \tilde{n}) = -\sum_{j=1}^{\infty} \frac{\Phi_{j2}^-(1) \Phi_{j1}^-(\tilde{n})}{\lambda_j^- \| \mathbf{\Phi}_j^- \|^2} + \frac{\Phi_{j2}^+(1) \Phi_{j1}^+(\tilde{n})}{\lambda_j^+ \| \mathbf{\Phi}_j^+ \|^2} + \sum_{j=1}^{\infty} \frac{\Phi_{j2}^+(1) \Phi_{j1}^+(\tilde{n})}{\lambda_j^+ \| \mathbf{\Phi}_j^+ \|^2} \exp(\lambda_j^+ \tilde{x}) \tag{33}$$

$$\tilde{x} > 0: \theta(\tilde{x}, \tilde{n}) = -\sum_{j=1}^{\infty} \frac{\Phi_{j2}^-(1) \Phi_{j1}^-(\tilde{n})}{\lambda_j^- \| \mathbf{\Phi}_j^- \|^2} \exp(\lambda_j^- \tilde{x}). \tag{34}$$

From equations (33) and (34) it can be observed that the solution for $\tilde{x} \leqslant 0$ contains both negative and positive eigenfunctions. By expanding the vector $(1, 0)^T$ into a set of orthonormal eigenfunctions according to equation (27) it can be shown that the first sum on the right-hand side of equation (33) is equal to 1. This leads to the following expression for the temperature distribution for $\tilde{x} \leqslant 0$

$$\tilde{x} \leqslant 0: \theta(\tilde{x}, \tilde{n}) = 1 + \sum_{j=1}^{\infty} \frac{\Phi_{j2}^+(1) \Phi_{j1}^+(\tilde{n})}{\lambda_j^+ \| \mathbf{\Phi}_j^+ \|^2} \exp(\lambda_j^+ \tilde{x}). \tag{35}$$

It should be noted that the continuity of $\theta(\tilde{x}, \tilde{n})$ at $\tilde{x} = 0$ is established immediately from the equations (33) and (34) and the boundary conditions for θ, equation (10), are obviously satisfied by equations (34) and (35). It can be shown from equation (23) that for $a_1(\tilde{n})/Pe_L^2 \to 0$ all λ_j^+ tend to infinity. Therefore, the solution for $\tilde{x} \leqslant 0$ tends to

$$\theta(\tilde{x}, \tilde{n}) = 1 \quad \text{for } a_1(\tilde{n})/Pe_L^2 \to 0 \tag{36}$$

which represents the solution of the limiting case which is the parabolic problem. The vector norm $\| \mathbf{\Phi}_j \|^2$, appearing in the solution, can be simplified by using the equations (21) and (22). It can be shown that the norm, given by equation (18), continuously approaches the norm for the parabolic problem if $a_1(\tilde{n})/Pe_L^2 \to 0$. Further it can be shown that

$$\| \mathbf{\Phi}_j \|^2 = \Phi_{j2}(1) \left. \frac{\mathrm{d}\Phi_j(1)}{\mathrm{d}\lambda} \right|_{\lambda_j}. \tag{37}$$

The reader is referred to Appendix 2 for more details concerning the vector norm. Introducing equation (37) into equations (34) and (35) results in the following equations describing the temperature distribution in the fluid

$$\tilde{x} \leqslant 0: \theta(\tilde{x}, \tilde{n}) = 1 + \sum_{j=1}^{\infty} A_j^+ \Phi_{j1}^+(\tilde{n}) \exp(\lambda_j^+ \tilde{x}) \tag{38}$$

$$\tilde{x} > 0: \theta(\tilde{x} n \tilde{n}) = \sum_{j=1}^{\infty} A_j^- \Phi_{j1}^-(\tilde{n}) \exp(\lambda_j \tilde{x}) \tag{39}$$

where the coefficients A_j are given by

$$A_j = (\lambda_j \, d\Phi_j(1)/d\lambda\,|_{\lambda_j})^{-1}. \quad (40)$$

For the designers of heat exchangers it is of great interest to know the axial variation of the Nusselt number. The Nusselt number, based on the hydraulic diameter of the duct, is defined by

$$Nu_D = -D\left(\frac{\partial T}{\partial n}\right)_{n=L} \Big/ (T_b - T_w). \quad (41)$$

The bulk temperature T_b appearing in equation (41) is given by

$$T_b = \int_0^1 uTr^k \, dn \Big/ \int_0^1 ur^k \, dn. \quad (42)$$

Introducing the dimensionless quantities given by equation (8) into the equations (41) and (42) and using the temperature distribution given by equations (38) and (39) results in the following expressions

different. A good literature review concerning the different models for the turbulent Prandtl number can be found in [15]. For the results presented here the model of Azer and Chao [16] was used because this model was able to predict relatively well the experimental results for the Nusselt number measured by Gilliland *et al.* [17] (taken from Reed [5]) and by Sleicher *et al.* [18]. The model for Pr_t derived by Azer and Chao [16] considers a simplified mechanism of turbulent heat transfer based on the mixing length hypothesis. It was assumed that there is a continuous change of momentum and energy during the flight of an eddy. Although their complete formulae for Pr_t are rather complicated, Azer and Chao [16] gave a simple approximation for the turbulent Prandtl number:

$$Pr_t = \frac{1 + 380/Pe_D^{0.58} \exp[-(1-\tilde{n})^{0.25}]}{1 + 135/Re_D^{0.45} \exp[-(1-\tilde{n})^{0.25}]}. \quad (48)$$

Additionally the assumption was made that the ratio of the axial diffusivity to the radial diffusivity $\varepsilon_{hx}/\varepsilon_{hn}$ appearing in equation (11) is equal to one. This assumption has been made previously by Lee [14] and by Chieng and Launder [19]. Nevertheless, it should be noted that the analysis presented in the previous section is more general and can be used with any turbulent Prandtl number concept and with arbitrary functions for $a_1(\tilde{n})$ and $a_2(\tilde{n})$.

$$\tilde{x} \leqslant 0: \theta_b = 1 + 2^k \sum_{j=1}^{\infty} A_j^+ \left\{ \frac{\Phi'^+_{j1}(1)}{\lambda_j^+} + \frac{\lambda_j^+}{Pe_L^2} \int_0^1 a_1(\tilde{n}) \Phi^+_{j1}(\tilde{n}) \tilde{r}^k \, d\tilde{n} \right\} \exp(\lambda_j^+ \tilde{x}) \quad (43)$$

$$\tilde{x} \leqslant 0: Nu_D = \frac{-4 \sum_{j=1}^{\infty} A_j^+ \Phi'^+_{j1}(1) \exp(\lambda_j^+ \tilde{x})}{4^k \sum_{j=1}^{\infty} A_j^+ \left\{ \frac{\Phi'^+_{j1}(1)}{\lambda_j^+} + \frac{\lambda_j^+}{Pe_L^2} \int_0^1 a_1(\tilde{n}) \Phi^+_{j1}(\tilde{n}) \tilde{r}^k \, d\tilde{n} \right\} \exp(\lambda_j^+ \tilde{x})} \quad (44)$$

$$\tilde{x} > 0: \theta_b = 2^k \sum_{j=1}^{\infty} A_j^- \left\{ \frac{\Phi'^-_{j1}(1)}{\lambda_j^-} + \frac{\lambda_j^-}{Pe_L^2} \int_0^1 a_1(\tilde{n}) \Phi^-_{j1}(\tilde{n}) \tilde{r}^k \, d\tilde{n} \right\} \exp(\lambda_j^- \tilde{x}) \quad (45)$$

$$\tilde{x} > 0: Nu_D = \frac{-4 \sum_{j=1}^{\infty} A_j^- \Phi'^-_{j1}(1) \exp(\lambda_j^- \tilde{x})}{4^k \sum_{j=1}^{\infty} A_j^- \left\{ \frac{\Phi'^-_{j1}(1)}{\lambda_j^-} + \frac{\lambda_j^-}{Pe_L^2} \int_0^1 a_1(\tilde{n}) \Phi^-_{j1}(\tilde{n}) r^k \, d\tilde{n} \right\} \exp(\lambda_j^- \tilde{x})}. \quad (46)$$

The Nusselt number for fully-developed flow can be derived from equation (46) by considering the limiting case $\tilde{x} \to \infty$

$$Nu_\infty = \frac{4\,|\lambda_1^-|}{4^k \left\{ 1 + \dfrac{\lambda_1^{-2}}{\Phi'^-_{11}(1) Pe_L^2} \displaystyle\int_0^1 a_1(\tilde{n}) \Phi^-_{11}(\tilde{n}) \tilde{r}^k \, d\tilde{n} \right\}}. \quad (47)$$

3. RESULTS AND DISCUSSION

In order to obtain solutions of the energy equation (9), the turbulent Prandtl number and the ratio $(\varepsilon_{hx}/\varepsilon_{hn})$ appearing in the equations (11) and (12) have to be specified. There is a variety of different models in the literature prescribing the turbulent Prandtl number. Especially in the case of liquid metal flows the values for Pr_t given by several models are quite

3.1. *Numerical procedure and accuracy of the predictions*

The eigenvalues λ_j as well as the eigenfunctions $\Phi_j(\tilde{n})$ were calculated numerically for the eigenvalue problem given by equation (23) by using a four-stage Runge–Kutta scheme. In order to examine the accuracy of the calculated values several calculations were carried out for laminar flows. The results for laminar pipe flow could be compared with the values given in Papoutsakis *et al.* [7] for different values of the Peclet

Table 1. Eigenvalues and constants for various Reynolds numbers and $Pr = 0.002$ (circular pipe)

		$Pr = 0.002$			
Re_D	n	$-\lambda_j^-$	A_j^-	λ_j^+	A_j^+
5000	1	4.1681E+00	1.3933E+00	3.4372E+01	−2.0427E−01
	2	1.6635E+01	−7.3175E−01	45841E+01	3.2643E−01
	3	3.1228E+01	5.2163E−01	6.0004E+01	−3.2597E−01
	4	4.6408E+01	−4.2075E−01	7.4956E+01	3.0601E−01
	5	6.1812E+01	3.6089E−01	9.0219E+01	−2.8529E−01
	6	7.7325E+01	−3.2067E−01	1.0564E+02	2.6687E−01
	7	9.2895E+01	2.9153E−01	1.2114E+02	−2.5097E−01
	8	1.0850E+02	−2.6922E−01	1.3670E+02	2.3729E−01
	9	1.2413E+02	2.5135E−01	1.5229E+02	−2.2544E−01
	10	1.3978E+02	−2.3669E−01	1.6790E+02	2.1509E−01
10000	1	4.7206E+00	1.5069E+00	1.1908E+02	−7.0578E−02
	2	2.2434E+01	−8.5318E−01	1.3678E+02	1.7954E−01
	3	4.7050E+01	6.0532E−01	1.5972E+02	−2.3428E−01
	4	7.4691E+01	−4.7805E−01	1.8658E+02	2.4440E−01
	5	1.0377E+02	4.0173E−01	2.1519E+02	−2.4155E−01
	6	1.3362E+02	−3.5094E−01	2.4472E+02	2.3439E−01
	7	1.6392E+02	3.1470E−01	2.7478E+02	−2.2599E−01
	8	1.9450E+02	−2.8747E−01	3.0518E+02	2.1752E−01
	9	2.2527E+02	2.6603E−01	3.3580E+02	−2.0942E−01
	10	2.5617E+02	−2.4871E−01	3.6659E+02	2.0185E−01
15000	1	4.8975E+00	1.5388E+00	2.5138E+02	−1.9053E−02
	2	2.4799E+01	−9.1289E−01	2.8039E+02	8.9513E−02
	3	5.5335E+01	6.6181E−01	3.0700E+02	−1.6288E−01
	4	9.2024E+01	−5.2373E−01	3.4161E+02	1.9182E−01
	5	1.3221E+02	4.3764E−01	3.8068E+02	−2.0131E−01
	6	1.7448E+02	−3.7939E−01	4.2220E+02	2.0291E−01
	7	2.1804E+02	3.3754E−01	4.6524E+02	−2.0084E−01
	8	2.6245E+02	−3.0603E−01	5.0925E+02	1.9703E−01
	9	3.0745E+02	2.8143E−01	5.5394E+02	−1.9245E−01
	10	3.5286E+02	−2.6166E−01	5.9910E+02	1.8758E−01

number. The eigenvalues calculated here agree for the case of laminar pipe flow ($a_1 = a_2 = 1$, $\tilde{u} = 2(1-\tilde{r}^2)$) within a relative error of $|\Delta\lambda_j|/|\lambda_j| < 10^{-7}$ while the calculated constants A_j were found to be in agreement with the values given by Papoutsakis *et al.* [7] within a relative error of $|\Delta A_j|/|A_j| < 10^{-6}$. In addition, the calculated values for eigenvalues are in very good agreement with those of Deavours [10] for laminar flow in a parallel plate channel.

3.2. *Heat transfer results for the circular pipe*

If the flow and heat transfer in a circular pipe is considered, the flow index k in the preceeding equations must be set to 1. Table 1 shows calculated eigenvalues λ_j as well as the constants A_j for different values of the Reynolds number and $Pr = 0.002$. The table contains values for $\tilde{x} > 0(\lambda_j^-, A_j^-)$ as well as the values for $\tilde{x} < 0(\lambda_j^+, A_j^+)$. From the table it can be seen that the positive eigenvalues increase dramatically with increasing Peclet numbers, indicating the vanishing influence of axial heat conduction for $\tilde{x} < 0$. According to Reed [5] only the experimental data of Sleicher *et al.* [18] and Gilliland *et al.* [17] (taken from Azer and Chao [16]) are judged to be reliable for the case of uniform wall temperature for the flow of liquid metals. Therefore, Fig. 2 shows a comparison between the author's predicted Nusselt numbers for fully-developed pipe flow and experimental data from [17] and [18]. It can be seen that the predicted Nusselt numbers for fully-developed flow are a little bit too low for higher values of the Peclet number, indicating that the turbulent Prandtl number model of Azer and Chao [16] underpredicts the values for the thermal mixing length for higher Peclet numbers. Nevertheless, for the range of Peclet numbers of interest ($Pe_D < 1000$) the model predicts

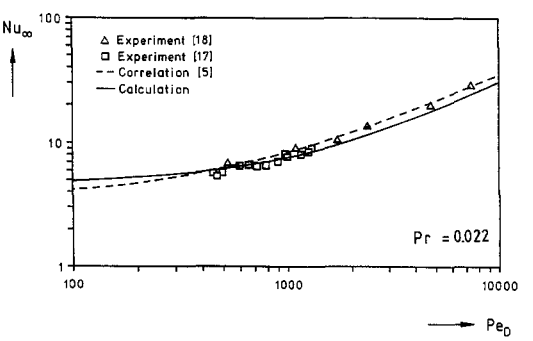

Fig. 2. Nusselt number for fully-developed pipe flow as a function of the Peclet number.

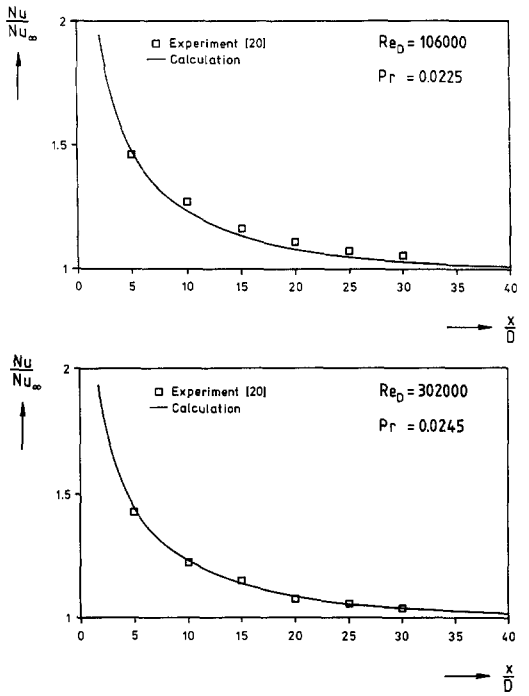

Fig. 3. Variation of the local Nusselt number in the thermal entry region of a circular pipe.

values for the Nusselt numbers which are in very good agreement with the measurements. In Fig. 2 the recommended Nusselt number relation of Reed [5] for constant wall temperature

$$Nu_D = 3.3 + 0.02 Pe_D^{0.8} \tag{49}$$

was also plotted. It can be seen that equation (49) represents a good fit to the data of Sleicher *et al.* [18] and Gilliland *et al.* [17]. Figure 3 shows a comparison between calculated values of the local Nusselt number, scaled by the Nusselt number for fully-developed flow, and experimental data from Awad [20]. It can be seen that the prediction compares well with the experimental results for both shown Reynolds numbers.

The preceeding calculations were carried out for a range of Peclet numbers where axial heat conduction in the fluid can be neglected with good accuracy. Let us now focus on low Peclet number flows. Unfortunately, there are no experimental data available by now for $Pe_D < 100$, but from the good agreement shown between calculations and measurements it can be expected that the turbulent Prandtl number model used will still give accurate results for Peclet numbers smaller than 100. Table 2 shows values for the Nusselt number for fully-developed flow for different Reynolds and Prandtl numbers. The values in brackets given in Table 2 indicate the Nusselt numbers for fully-developed flow for the case of $a_1(\tilde{n})/Pe_D^2 \to 0$ (no axial heat conduction, parabolic problem). As it was noted before by Lee [14], it can be seen that the effect of axial heat conduction is negligible for thermally fully-developed flow. It was shown by Papoutsakis *et al.* [7] that the Nusselt number for fully-developed flow does not depend on the upstream wall boundary conditions ($\tilde{x} < 0$). This fact makes it possible to compare the here predicted Nusselt numbers *for thermally fully-developed flow* with the Nusselt numbers given by Lee [14] although the boundary conditions for $\tilde{x} < 0$ are competely different. It was found that the values for the Nusselt number for the thermally fully-developed flow agree within a relative error of less than 1.5% with the values given by Lee [14].

One other interesting fact can be recognized from Table 2. For very low values of the Reynolds number ($Re_D = 3000$, $Re_D = 5000$) the value of the Nusselt number for fully-developed flow first decreases with increasing values of the Prandtl number and subsequently increases with increasing Pr. This is due to the fact that for this low values of Re_D the functions $a_1 = a_2 \cong 1$ for very low values of Pr. Therefore, the fully-developed Nusselt number starts to behave as for laminar flow showing the typical increase of Nu_∞ with decreasing values of the Peclet numbers [4]. With increasing Prandtl numbers the functions a_1 and a_2 start to deviate from unity, which means that the eddy diffusivity reaches higher values and therefore the Nusselt number for fully-developed flow starts to increase.

Figure 4 shows the effect of axial heat conduction in the flow on the distribution of the local Nusselt number for two different Peclet numbers. The Nusselt numbers are plotted as a function of the modified axial coordinate $x/(DPe_D)$. For $Pe_D = 10$ it can be seen that a pronounced difference exists between the

Table 2. Nusselt numbers for fully developed flow in a circular pipe ($\tilde{x} \to \infty$) as a function of the Reynolds and Prandtl number. The values in brackets indicate the Nusselt numbers for fully developed flow without axial heat conduction effects

	Pr				
Re_D	0.002	0.004	0.006	0.01	0.02
3000	4.635(4.576)	4.601(4.580)	4.595(4.585)	4.601(4.597)	4.643(4.642)
5000	4.763(4.737)	4.752(4.745)	4.758(4.755)	4.782(4.781)	4.872(4.872)
8000	4.871(4.859)	4.877(4.874)	4.895(4.893)	4.944(4.943)	5.113(5.113)
10000	4.917(4.910)	4.931(4.929)	4.956(4.955)	5.022(5.022)	5.247(5.247)
15000	4.993(4.989)	5.024(5.022)	5.067(5.067)	5.178(5.178)	5.548(5.548)
20000	5.042(5.040)	5.089(5.088)	5.152(5.152)	5.310(5.310)	5.832(5.832)
30000	5.109(5.108)	5.189(5.189)	5.293(5.293)	5.553(5.553)	6.384(6.384)

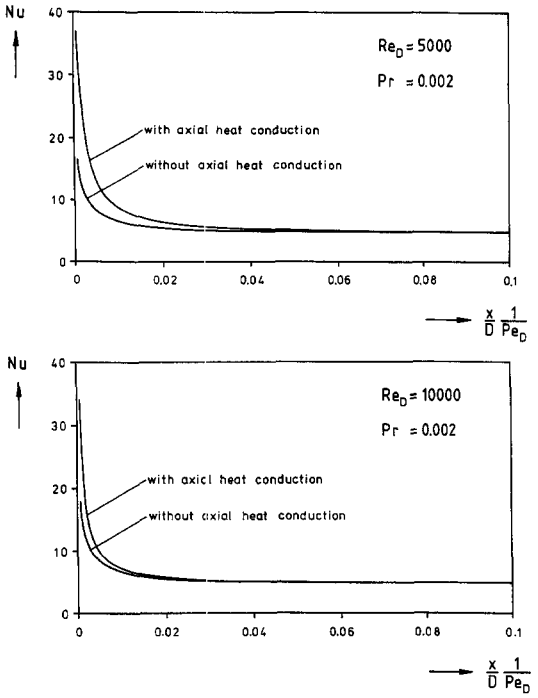

Fig. 4. Effect of axial heat conduction on the shape of the local Nusselt number.

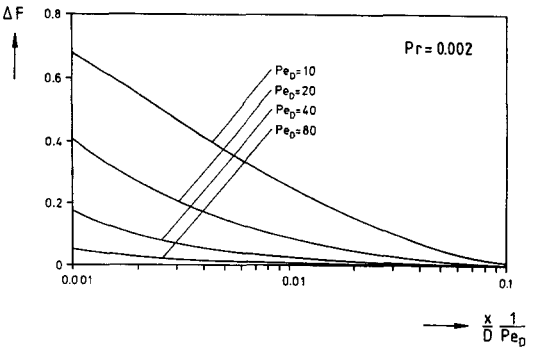

Fig. 5. Relative error in the local Nusselt number due to ignoring the axial heat conduction with the fluid (circular pipe).

Nusselt number for the case with axial heat conduction and the parabolic calculation (no axial heat conduction). It can be observed that the Nusselt number for the case with axial heat conduction is higher than the related Nusselt number for the parabolic problem. This is in accordance with the results of Hennecke [12] for laminar pipe flow. Furthermore the figure shows that the thermal entrance length is enlarged by considering axial heat conduction within the fluid. For $Pe_D = 20$ it can be seen that the effect of axial heat conduction is less important for the shape of the Nusselt number. Additionally the thermal entrance length is for $Pe_D = 20$ very similar for the two cases with and without axial heat conduction. It should be pointed out here that because of the slow convergence of the series for the Nusselt number, equation (46), a lot of eigenvalues have to be taken to guarantee sufficiently accurate results for the case of Dirichlet boundary conditions. For $x/(DPe_D) > 10^{-3}$ and Peclet numbers bigger than 10 for example about 100 eigenvalues and eigenfunctions are required to guarantee accurate results.

Figure 5 shows the relative error ΔF in the Nusselt number due to ignoring axial heat conduction effects within the fluid. As expected, the relative error increases with decreasing values of the Peclet number and decreasing values of the axial coordinate. Nevertheless, the shape of the curves as well as the magnitude of the relative error are quite different to those predicted by Lee [14]. For $Pe_D = 10$, Lee [14] predicted a maximum error of about 32% occurring at $x/(DPe_D) \approx 0.002$. For lower values of the axial coordinate the relative error was decreasing. In the present study it was found that the relative error was gradually increasing for decreasing values of the axial coordinate. This different behaviour is due to the differrent boundary conditions used in the present study. Lee [14] used for his study an adiabatic entry length for $\tilde{x} < 0$ and a constant wall temperature for $\tilde{x} > 0$, whereas in the present study Dirichlet boundary conditions were used. It can be stated that the effect of axial heat conduction on the Nusselt number will be more pronounced for Dirichlet boundary conditions than for the insulated upstream region investigated by Lee [14]. Additionally it has to be noted that Lee [14] used only 20 eigenvalues and eigenfunctions for his calculations. Because he applied no Dirichlet boundary conditions, the number of terms might be enough for most of his calculations. Nevertheless, it is questionable if the shape of the relative error for very low Peclet numbers ($Pe_D = 5$) and very small values of the axial coordinate could be calculated with sufficient accuracy by him. The following Fig. 6 shows the temperature distribution within the fluid for several axial locations. For $\tilde{x} > 0$ the well-known shape of the temperature profile can be observed. The fluid continuously loses heat and the temperature of the flow aproaches the wall temperature for $\tilde{x} \to \infty$. Additionally Fig. 6 shows several temperature distributions for negative axial coordinates which elucidate the effect of axial heat conduction. The region of influence of axial heat conduction for the two different values of the Peclet numbers can be clearly seen from Fig. 6.

3.3. *Heat transfer results for the parallel plate channel*

For flow and heat transfer in a parallel plate channel, the flow index k in the preceeding equations must be set to 0. Table 3 shows calculated eigenvalues λ_j as well as the constants A_j for different values of the Reynolds number and $Pr = 0.001$. Table 4 shows values of the Nusselt number for fully developed flow in a parallel plate channel for various values of the Reynolds and Prandtl number. Similar to Table 2, the values in brackets indicate the Nusselt numbers for

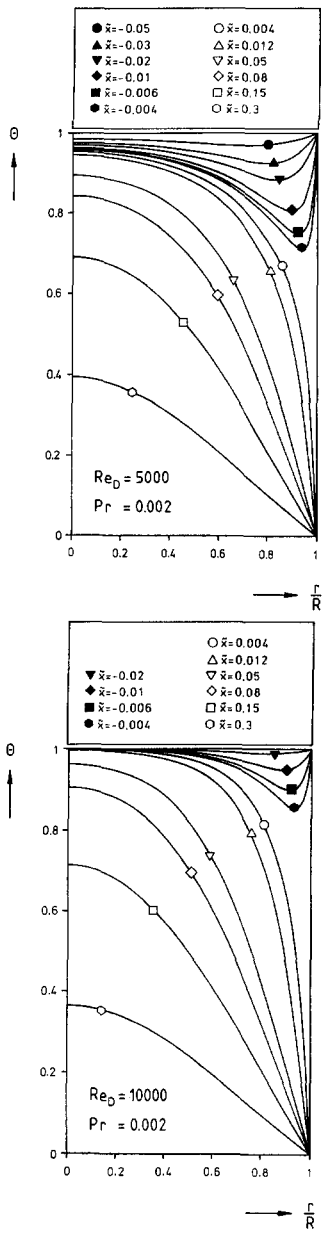

Fig. 6. Development of the temperature distribution in the thermal entry region of a circular pipe.

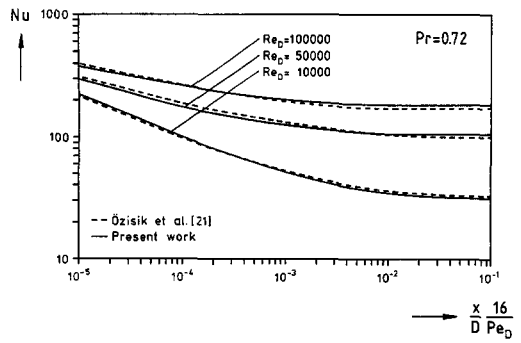

Fig. 7. Local Nusselt number in the thermal entry region of a parallel plate channel for $Pr = 0.72$.

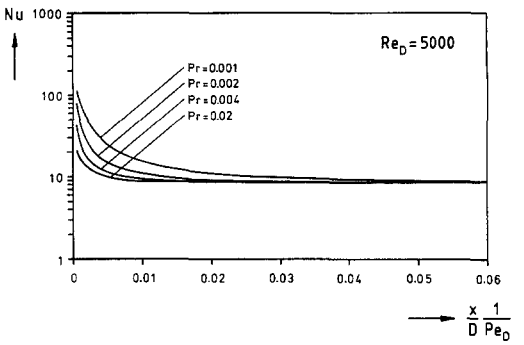

Fig. 8. Influence of the Prandtl number on the shape of the local Nusselt number in a parallel plate channel.

the case of neglected axial heat conduction (parabolic problem).

Figure 7 shows the distribution of the local Nusselt number in the thermal entrance region of a parallel plate channel for air ($Pr = 0.71$). In addition, the figure contains calculated local Nusselt numbers from Özisik *et al.* [21] which are in good agreement with existing correlations. From Fig. 7 it can be seen that the present calculations are in very good agreement with the results of [21], which might be seen as another check of the validity of the present calculations. For the predictions shown in Fig. 7 the turbulent Prandtl number concept of Kays and Crawford [23] was used because equation (48) is only valid for liquid metals.

Figure 8 displays the effect of axial heat conduction within the fluid on the distribution of the local Nusselt number for a given value of the Reynolds number. It can be seen that decreasing values of the Prandtl number result in an increasing value of the Nusselt number in the thermal entrance region. Additionally it can be observed that the length of the thermal entrance region is enlarged by decreasing the Peclet number. This shows very clearly the effect of axial heat conduction within the fluid on the shape of the Nusselt number for Dirichlet wall boundary conditions. Figure 9 displays the relative error in the Nusselt number due to ignoring axial heat conduction effects within the fluid. The shape of the curves are quite similar to

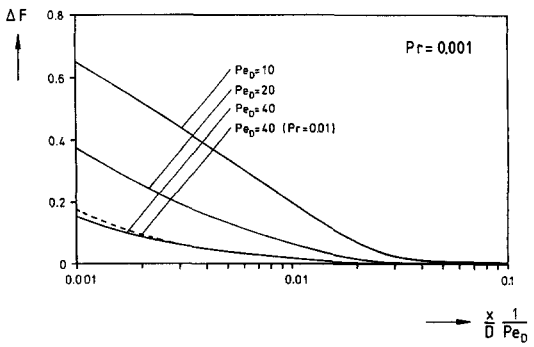

Fig. 9. Relative error in the local Nusselt number due to ignoring the axial heat conduction within the fluid (parallel plate channel).

Table 3. Eigenvalues and constants for various Reynolds numbers and $Pr = 0.001$ (parallel plate channel)

		$Pr = 0.001$			
Re_D	n	$-\lambda_j^-$	A_j^-	λ_j^+	A_j^+
10000	1	1.7507E+00	1.0431E+00	8.7937E+00	−2.3077E−01
	2	8.9611E+00	−2.5446E−01	1.5488E+01	1.7069E−01
	3	1.6690E+01	1.4051E−01	2.3103E+01	−1.1420E−01
	4	2.4496E+01	−9.6905E−02	3.0853E+01	8.4945E−02
	5	3.2325E+01	7.4002E−02	3.8648E+01	−6.7412E−02
	6	4.0164E+01	−5.9896E−02	4.6464E+01	5.5798E−02
	7	4.8008E+01	5.0331E−02	5.4292E+01	−4.7562E−02
	8	5.5854E+01	−4.3417E−02	6.2127E+01	4.1425E−02
	9	6.3702E+01	3.8182E−02	6.9967E+01	−3.6680E−02
	10	7.1551E+01	−3.4080E−02	7.7810E+01	3.2905E−02
15000	1	1.9645E+00	1.1253E+00	1.7605E+01	−1.4890E−01
	2	1.1812E+01	−2.7523E−01	2.6446E+01	1.5031E−01
	3	2.3116E+01	1.4822E−01	3.7538E+01	−1.0654E−01
	4	3.4698E+01	−1.0070E−01	4.9014E+01	8.1150E−02
	5	4.6372E+01	7.6178E−02	6.0623E+01	−6.5222E−02
	6	5.8087E+01	−6.1270E−02	7.2293E+01	5.4407E−02
	7	6.9823E+01	5.1259E−02	8.3996E+01	−4.6617E−02
	8	8.1572E+01	−4.4075E−02	9.5721E+01	4.0750E−02
	9	9.3328E+01	3.8667E−02	1.0746E+02	−3.6180E−02
	10	1.0509E+02	−3.4448E−02	1.1921E+02	3.2521E−02
20000	1	2.0705E+00	1.1696E+00	2.9631E+01	−1.0488E−01
	2	1.3929E+01	−2.9336E−01	3.9890E+01	1.3243E−01
	3	2.8509E+01	1.5563E−01	5.4128E+01	−9.9146E−02
	4	4.3718E+01	−1.0450E−01	6.9172E+01	7.7329E−02
	5	5.9151E+01	7.8424E−02	8.4502E+01	−6.2954E−02
	6	7.4687E+01	−6.2723E−02	9.9966E+01	5.2936E−02
	7	9.0277E+01	5.2259E−02	1.1550E+02	−4.5600E−02
	8	1.0590E+02	−4.4794E−02	1.3109E+02	4.0015E−02
	9	1.2154E+02	3.9204E−02	1.4670E+02	−3.5629E−02
	10	1.3720E+02	−3.4860E−02	1.6233E+02	3.2096E−02

Table 4. Nusselt numbers for fully developed flow in a parallel plate channel as a function of the Reynolds and Prandtl number. The values in brackets indicate the Nusselt numbers for fully developed flow without axial heat conduction effects

	Pr				
Re_D	0.002	0.004	0.006	0.01	0.02
3000	8.370(8.253)	8.304(8.255)	8.284(8.258)	8.277(8.267)	8.298(8.295)
5000	8.518(8.462)	8.486(8.468)	8.484(8.475)	8.497(8.494)	8.560(8.559)
8000	8.686(8.662)	8.680(8.673)	8.691(8.688)	8.728(8.727)	8.859(8.859)
10000	8.760(8.744)	8.765(8.760)	8.783(8.781)	8.835(8.834)	9.017(9.017)
15000	8.858(8.851)	8.881(8.879)	8.917(8.916)	9.010(9.010)	9.326(9.326)
20000	8.919(8.915)	8.957(8.956)	9.011(9.011)	9.149(9.149)	9.608(9.608)
30000	9.012(9.010)	9.082(9.082)	9.175(9.175)	9.408(9.408)	10.164(10.164)

the ones plotted in Fig. 5 for pipe flow. Nevertheless, by comparing Fig. 9 with Fig. 5 it can be noticed that the region of influence of axial heat conduction is smaller for the parallel plate channel than for the pipe. This is due to the fact that the thermal entry length L_{th} for a parallel plate channel scaled by D and Pe_D is much smaller than for pipe flow. For laminar flow and neglected effects of axial heat conduction for example $L_{th}/(DPe_D) = 0.03346$ for pipe flow and only 0.00797 for a parallel plate channel [4].

4. CONCLUSIONS

According to the present analytical study concerning the influence of axial heat conduction within the fluid, the following major conclusions can be drawn:

(1) By using a new defined vector norm it is possible to obtain a selfadjoint eigenvalue problem for the extended turbulent Graetz problem even though the original convective diffusion operator is nonself-

adjoint. Therefore, an entirely analytical solution to the extended turbulent Graetz problem with Dirichlet wall boundary conditions could be developed.

(2) The obtained analytical results for pipe flow are compared with measurements of Gilliland *et al.* [17] and Sleicher *et al.* [18] and good agreement between measured and computed Nusselt numbers could be observed.

(3) The relative error in Nusselt number due to ignoring the effect of axial heat conduction in the fluid is very much dependent on the kind of wall boundary conditions. For Dirichlet wall boundary conditions the relative error reaches maximum values.

(4) For very small Peclet numbers it can be observed that the fully developed Nusselt number increases with decreasing Peclet numbers and behaves as for laminar flow.

Finally it should be noted that the shown solution method with the defined norm by equation (18) can be used for a broad class of problems associated with partial differential equations similar to equation (1). Related problems with additional source terms in equation (1) can be solved in a similar way. The reader is referred to Weigand *et al.* [11] where an example is given on how to incorporate additional source terms into the solution for the case of laminar flow in a parallel plate channel.

Acknowledgements—The interesting and helpful discussions with Professor Dr-Ing. H. Beer (TH Darmstadt, Germany) concerning the present work are gratefully acknowledged.

REFERENCES

1. L. Graetz, Über die Wärmeleitungsfähigkeit von Flüssigkeiten, Teil 1, *Ann. Phys. Chem.* **18,** 79–84 (1883).
2. L. Graetz, Über die Wärmeleitfähigkeit von Flüssigkeiten, Teil 2, *Ann. Phys. Chem.* **25,** 337–357 (1885).
3. W. Nusselt, Die Abhängigkeit der Wärmeübergangszahl von der Rohrlänge, *VDI Zeitschrift* **54,** 1154–1158 (1910).
4. R. K. Shah and A. L. London, *Laminar Flow Force Convection in Ducts*, Chaps. V and VI. Academic Press, New York (1978).
5. C. B. Reed, Convective heat transfer in liquid metals. In *Handbook of Single-phase Convective Heat Transfer* (Edited by S. Kakac, R. K. Shah and W. Aung), Chap. 8. Wiley, New York (1987).
6. C. J. Hsu, An exact analysis of low Peclet number thermal entry region heat transfer in transversally nonuniform velocity fields, *A.I.Ch.E.Jl* **17,** 732–740 (1971).
7. E. Papoutsakis, D. Ramkrishna and H. C. Lim, The extended Graetz problem with Dirichlet wall boundary conditions, *Appl. Sci. Res.* **36,** 13–34 (1980).
8. D. Ramkrishna and N. R. Amundson, Boundary value problems in transport with mixed and oblique derivative boundary conditions—II. Reduction to first order systems, *Chem. Engng Sci.* **34,** 309–318 (1979).
9. M. A. Ebadin and H. Y. Zhang, An exact solution of extended Graetz problem with axial heat conduction, *Int. J. Heat Mass Transfer* **32,** 1709–1717 (1989).
10. C. A. Deavours, An exact solution for the temperature distribution in parallel plate Poiseuille flow. *J. Heat Transfer* **96,** 489–495 (1974).
11. B. Weigand, J. Schmidt and H. Beer, An analytic study of liquid solidification in low Peclet number forced flows inside a parallel plate channel concerning axial heat conduction, *Proceedings of the Fourth International Symposium on Thermal Engineering Science for Cold Regions*, pp. 39–47 (1993).
12. D. K. Hennecke, Heat transfer by Hagen-Poiseuille flow in the thermal development region with axial conduction, *Wärme-und Stoffübertragung* **1,** 177–184 (1968).
13. T. V. Nguyen, Laminar heat transfer for thermally developing flow in ducts, *Int. J. Heat Mass Transfer* **35,** 1733–1741 (1992).
14. S. L. Lee, Forced convection heat transfer in low Prandtl number turbulent flows: influence of axial conduction, *Can. J. Chem. Engng* **60,** 482–486 (1982).
15. A. J. Reynolds, The prediction of turbulent Prandtl and Schmidt numbers, *Int. J. Heat Mass Transfer* **18,** 1055–1069 (1975).
16. N. Z. Azer and B. T. Chao, A mechanism of turbulent heat transfer in liquid metals, *Int. J. Heat Mass Transfer* **1,** 121–138 (1960).
17. E. R. Gilliland, R. J. Musser and W. R. Page, Heat transfer to mercury, *General Discussion on Heat Transfer*, pp. 402–404. Institution of Mechanical Engineers and ASME, London (1951).
18. C. A. Sleicher, A. S. Awad and R. H. Notter, Temperature and eddy diffusivity profiles in NaK, *Int. J. Heat Mass Transfer* **16,** 1565–1575 (1973).
19. C. C. Chieng and B. E. Launder, On the calculation of turbulent heat transfer downstream from an abrupt pipe expansion, *Number Heat Transfer* **3,** 189–207 (1980).
20. A. S. Awad, Heat transfer and eddy diffusivity in NaK in a pipe at uniform wall temperature, Ph.D. Thesis, University of Washington, Seattle (1965).
21. M. N. Özisik, R. M. Cotta and W. S. Kim, Heat transfer in turbulent forced convection between parallel-plates, *Can. J. Chem. Engng* **67,** 771–776 (1989).
22. S. Faggiani and F. Gori, Influence of streamwise molecular heat conduction on the heat transfer for liquid metals in turbulent flow between parallel plates, *J. Heat Transfer* **102,** 292–296 (1980).
23. W. M. Kays and M. E. Crawford, *Convective Heat and Mass Transfer*, Chap. 13. McGraw-Hill, New York (1993).

APPENDIX 1

In this Appendix it will be shown that the eigenfunctions related to equation (20) constitute a set of orthonormal functions. Consider the two eigenvectors $\mathbf{\Phi}_j$ and $\mathbf{\Phi}_k$ with the related eigenvalues λ_j and λ_k. From equation (20) one gets

$$\mathbf{L}\mathbf{\Phi}_j = \lambda_j \mathbf{\Phi}_j \quad \mathbf{L}\mathbf{\Phi}_k = \lambda_k \mathbf{\Phi}_k \tag{A1}$$

with the boundary conditions

$$\Phi_{j1}(1) = \Phi_{k1}(1) = 0 \quad \Phi_{j2}(0) = \Phi_{k2}(0) = 0. \tag{A2}$$

By taking the inner product of both sides of equations (A1) according to equation (18) the following expression is obtained

$$\langle \mathbf{L}\mathbf{\Phi}_j, \mathbf{\Phi}_k \rangle - \langle \mathbf{\Phi}_j, \mathbf{L}\mathbf{\Phi}_k \rangle = (\lambda_j - \lambda_k)\langle \mathbf{\Phi}_j, \mathbf{\Phi}_k \rangle. \tag{A3}$$

Because the operator L is a symmetric operator in the Hilbert space H of interest (this means that $\langle \mathbf{\Phi}, \mathbf{L}\Lambda \rangle = \langle \mathbf{L}\mathbf{\Phi}, \Lambda \rangle$) it follows from equation (A3)

$$\langle \mathbf{\Phi}_j, \mathbf{\Phi}_k \rangle = \begin{cases} 0 & \text{for } \lambda_j \neq \lambda_k \\ \| \mathbf{\Phi}_j \|^2 & \text{for } \lambda_j = \lambda_k \end{cases}. \tag{A4}$$

This of course shows that the eigenfunctions constitute a set of orthogonal functions for the inner product defined by equation (18).

APPENDIX 2

In this Appendix some interesting results concerning the vector norm $\| \Phi_j \|^2$ will be discussed. The vector norm is defined by equation (18) as

$$\| \Phi_j \|^2 = \langle \Phi_j, \Phi_j \rangle = \int_0^1 \left\{ \frac{a_1(\tilde{n}) \tilde{r}^k}{Pe_L^2} \Phi_{j1}^2(\tilde{n}) + \frac{1}{a_2(\tilde{n}) \tilde{r}^k} \Phi_{j2}^2(\tilde{n}) \right\} d\tilde{n} \tag{A5}$$

with $\Phi_{j1}(1) = \Phi_{j2}(0) = 0$. Using equations (21) and (22) and integrating the second part of the integral by parts, the following result for the vector norm can be obtained

$$\| \Phi_j \|^2 = -\frac{1}{\lambda_j} \int_0^1 \tilde{r}^k \tilde{u} \Phi_{j1}^2 \, d\tilde{n} + \frac{2}{Pe_L^2} \int_0^1 \tilde{r}^k a_1(\tilde{n}) \Phi_{j1}^2 \, d\tilde{n}. \tag{A6}$$

Equation (A6) shows the very interesting result that the vector norm approaches continuously the norm for the parabolic problem for $a_1(\tilde{n})/Pe_L^2 \to 0$ (note that $\lambda_j = -|\lambda_j|$ for $\tilde{x} > 0$).

Finally equation (37) will be derived. Consideration is given to the two eigenvectors Φ_j and Φ satisfying equation (20).

$$\mathbf{L}\Phi_j = \lambda_j \Phi_j \quad \mathbf{L}\Phi = \lambda \Phi \tag{A7}$$

with the boundary conditions

$$\Phi_{j1}(1) = \Phi_{j2}(0) = 0 \quad \Phi_2(0, \lambda) = 0. \tag{A8}$$

Further it will be assumed that

$$\lim_{\lambda \to \lambda_j} \Phi(\tilde{n}, \lambda) = \Phi_j(\tilde{n}). \tag{A9}$$

Taking the inner product of both sides of equation (A7) according to equation (18) the following equation can be obtained

$$(\lambda - \lambda_j) \langle \Phi_j, \Phi(\tilde{n}, \lambda) \rangle = \Phi_{j2}(1) \Phi_1(1, \lambda). \tag{A10}$$

By using the rule of de l'Hospital it can be shown that equation (A10) is equal to equation (37).